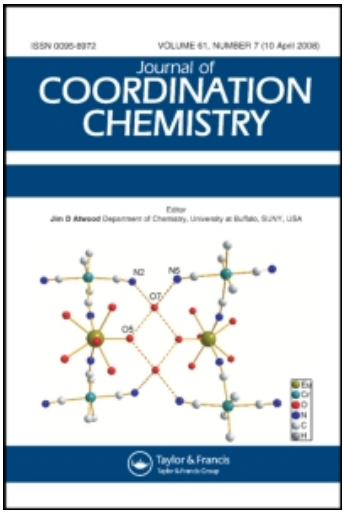

Journal of Coordination Chemistry

Publication details, including instructions for authors and subscription information:
http://www.informaworld.com/smpp/title~content=t713455674

Synthesis, characterization and antimicrobial activities of transition metal complexes of N,N-dialkyl-N'-(2-chlorobenzoyl)thiourea derivatives

Gün Binzet[a]; Hakan Arslan[a]; Ulrich Flörke[b]; Nevzat Külcü[a]; Nizami Duran[c]
[a] Faculty of Arts and Sciences, Department of Chemistry, Mersin University, Mersin, Turkey [b] Department of Chemistry, University of Paderborn, Paderborn, Germany [c] Faculty of Medicine, Department of Microbiology, Mustafa Kemal University, Hatay, Turkey

To cite this Article Binzet, Gün , Arslan, Hakan , Flörke, Ulrich , Külcü, Nevzat and Duran, Nizami(2006) 'Synthesis, characterization and antimicrobial activities of transition metal complexes of **N,N**-dialkyl-**N'**-(2-chlorobenzoyl)thiourea derivatives', Journal of Coordination Chemistry, 59: 12, 1395 — 1406
To link to this Article: DOI: 10.1080/00958970500512633
URL: http://dx.doi.org/10.1080/00958970500512633

Journal of Coordination Chemistry
Vol. 59, No. 12, 5 August 2006, 1395–1406

Taylor & Francis
Taylor & Francis Group

Synthesis, characterization and antimicrobial activities of transition metal complexes of *N*,*N*-dialkyl-*N*′-(2-chlorobenzoyl)thiourea derivatives

GÜN BINZET†, HAKAN ARSLAN*†, ULRICH FLÖRKE‡, NEVZAT KÜLCÜ† and NIZAMI DURAN§

†Faculty of Arts and Sciences, Department of Chemistry, Mersin University, Mersin, Turkey
‡Department of Chemistry, University of Paderborn, Paderborn, Germany
§Faculty of Medicine, Department of Microbiology, Mustafa Kemal University, Hatay, Turkey

(*Received in final form 10 October 2005*)

N,*N*-di-*n*-propyl-*N*′-(2-chlorobenzoyl)thiourea (HL^1) (**1**), *N*,*N*-diphenyl-*N*′-(2-chlorobenzoyl) thiourea (HL^2) (**2**), and their Ni^{II}, Co^{II}, Cu^{II}, Zn^{II}, Pt^{II}, Cd^{II} and Pd^{II} complexes have been synthesized and characterized. HL^1 and its copper complex were characterized by single-crystal X-ray diffraction methods. The ligands coordinate as bidentates yielding essentially neutral complexes of the type $[ML_2]$. The complexes were screened for their *in vitro* antibacterial, antifungal activities and toxicity. All compounds showed antimicrobial activity, but antibacterial efficacy is greater than antifungal activity.

Keywords: Benzoylthiourea; Complex; Crystal structure; Antimicrobial activity

1. Introduction

Thiourea derivatives and their transition metal complexes have been known for over a century and are easily synthesized in good yields. Thiourea derivatives have recently attracted interests in view of the potential use of these compounds as highly selective reagents for the pre-concentration and separation of metal cations in different matrices [1]. Thermal behaviour and decomposition kinetics of metal complexes have been reported [2–6]. Biological activities of complexes have been well documented and derivatives have been successfully screened for various actions; some have been used in commercial fungicides [7–9].

*Corresponding author. Email: arslanh@mersin.edu.tr

Journal of Coordination Chemistry
ISSN 0095-8972 print: ISSN 1029-0389 online © 2006 Taylor & Francis
DOI: 10.1080/00958970500512633

We have pursued characterization and antimicrobial activity of several new thiourea derivatives [2–6, 10–15]. In this article, we report the preparation, characterization and antimicrobial activities of *N*,*N*-di-*n*-propyl-*N*′-(2-chlorobenzoyl)thiourea (HL^1) (**1**), *N*,*N*-diphenyl-*N*′-(2-chlorobenzoyl)thiourea (HL^2) (**2**) and some of their transition metal complexes. The crystal structures of *N*,*N*-di-*n*-propyl-*N*′-(2-chloro-benzoyl) thiourea (**1**) and its copper complex are described.

2. Experimental

FTIR (KBr pellets) spectra were recorded on a Shimadzu 435 spectrophotometer between 4000 and 400 cm^{-1}. Electronic spectra (dichloromethane solutions) were recorded on a Shimadzu UV1601 spectrophotometer. ^1H NMR spectra were recorded on a Bruker DPX 300 spectrometer, using $CDCl_3$ as solvent and TMS as internal standard. Mass spectra were recorded on a VG Autospec, with FAB and EI techniques. C, H and N analyses were carried out on a Carlo Erba MOD 1106 instrument. Room temperature magnetic susceptibility measurements were carried out using a Sherwood-Scientific Gouy magnetic balance (Calibrant: $Hg[Co(SCN)_4]$). DTA and TG curves were obtained with a Shimadzu DT40 instrument with a heating rate of 10 K min^{-1}, nitrogen atmosphere, flow rate 60 cm^3 min^{-1}, platinum crucible, sample size 5 to 8 mg, reference α-Al_2O_3. X-ray powder diffraction analyses of final residues were made with a Siemens F diffractometer using Cu Kα radiation ($\lambda = 1.5406$ Å).

Single crystal X-ray data were collected on a Bruker AXS P4 diffractometer for L^1H and $Cu(L^1)_2$ using monochromated Mo-Kα radiation at 203(2) K. Three standard reflections monitored after every 300 reflections showed only random deviations. LP and empirical absorption (only for $Cu(L^1)_2$) corrections via psi-scans were applied. The structures were solved by direct and conventional Fourier methods. Full-matrix least-squares refinements were based on F^2. All non-hydrogen atoms were refined anisotropically; geometrically placed hydrogen atoms were refined with a 'riding model' and $U(H) = 1.2\,U(C_{iso})$ ($1.5\,U(C_{iso})$ for methyl groups) using SHELXTL [16]. Further details concerning data collection and refinement are given in table 1.

2.1. *Synthesis of ligands*

All chemicals used were of reagent grade quality. Some of the solvents were distilled before use. The ligands were prepared by a procedure similar to that reported in the literature [11, 17]. A solution of 2-chlorobenzoyl chloride (0.01 mol) in acetone (50 cm^3) was added dropwise to a suspension of potassium thiocyanate (0.01 mol) in acetone (30 cm^3). The reaction mixture was heated under reflux for 30 min, then cooled to room temperature. A solution of secondary amine (0.01 mol) in acetone (10 cm^3) was added and the resulting mixture stirred for 2 h. Hydrochloric acid (0.1 M, 300 cm^3) was added and the solution filtered. The solid product was washed with water and purified by recrystallization from ethanol : dichloromethane (1 : 1).

2.1.1. *N*,*N*-di-*n*-propyl-*N*′-(2-chlorobenzoyl)thiourea (HL^1). White. Yield: 79%, m.p. 69–71°C. Anal. Calcd for $C_{14}H_{19}N_2OSCl$ (%): C, 56.3; H, 6.4; N, 9.4. Found: C, 56.3;

Table 1. Summary of crystallographic data and refinement parameters for the HL^1 and $Cu(L^1)_2$.

	HL^1	$Cu(L^1)_2$
Empirical formula	$C_{14}H_{19}ClN_2OS$	$C_{28}H_{36}C_{12}CuN_4O_2S_2$
Formula weight	298.82	659.17
Temperature (K)	203(2)	203(2)
Wavelength (Å)	0.71073	0.71073
Crystal system	Triclinic	Monoclinic
Space group	$P\bar{1}$	$P2_{1/n}$
Unit cell dimensions		
a (Å)	7.886(1)	10.019(6)
b (Å)	14.095(2)	21.790(4)
c (Å)	15.208(2)	14.872(3)
α (°)	74.59(1)	90
β (°)	76.86(1)	100.09(3)
γ (°)	85.56(1)	90
V (Å^3)	1586.7(4)	3197(2)
Z	4	4
D_c (Mg m^{-3})	1.251	1.370
Absorption coefficient (mm^{-1})	0.367	1.012
$F(000)$	632	1372
Crystal size (mm)^3	$0.48 \times 0.25 \times 0.20$	$0.50 \times 0.14 \times 0.10$
θ range for data collection (°)	2.85 to 27.50	2.33 to 27.50
Index ranges	$-10 \le h \le 1$ $-17 \le k \le 17$ $-19 \le l \le 19$	$-1 \le h \le 13$ $-28 \le k \le 1$ $-19 \le l \le 9$
Reflections collected	8772	9014
Independent reflections (R_{int})	7209(0.0181)	7331(0.0491)
Absorption correction	None	Psi-scans
Refinement method	Full-matrix least-squares on F^2	Full-matrix least-squares on F^2
Data/parameters	7209/370	7331/353
Goodness-of-fit on F^2	1.108	0.962
Final R indices [$I > 2\sigma(I)$]	$R_1 = 0.0910$, $wR_2 = 0.2287$	$R_1 = 0.0952$, $wR_2 = 0.2471$
R indices (all data)	$R_1 = 0.1238$, $wR_2 = 0.2462$	$R_1 = 0.2181$, $wR_2 = 0.3737$
Largest diff. peak and hole (e Å^{-3})	0.701 and −0.629	0.867 and −0.544

H, 6.5; N, 9.5. IR (cm^{-1}): ν(N–H) 3138 (br), ν(C=O) 1690 (s), ν(C–Cl) 739 (w). ^{1}H NMR: δ 8.76 (s, 1H, NH), 7.60 (d, 1H, C_6H_4Cl), 7.43–7.31 (m, 3H, C_6H_4Cl), 3.88 (t, 2H, CH_2), 3.58 (t, 2H, CH_2), 1.88–1.66 (m, 4H, CH_2), 0.99–0.91 (m, 6H, CH_3). MS(EI), m/z(%) = 298 (M,60), 263 (100), 207 (19), 139 (78), 111 (28), and 43 (54). Electronic spectrum, λ_{max} (cm^{-1}): 42373, 34843, 27855.

2.1.2. *N*,*N*-diphenyl-*N′*-(2-chlorobenzoyl)thiourea, (HL^2). Yellow. Yield: 90%, m.p. 165–167°C. Anal. Calcd for $C_{20}H_{15}N_2OSCl$ (%): C, 65.5; H, 4.1; N, 7.6. Found: C, 65.7; H, 4.2; N, 7.8 IR (cm^{-1}): ν(N–H) 3158 (br), ν(C=O) 1694 (s), ν(C–Cl) 748 (w). ^{1}H NMR: δ 8.86 (s, 1H, NH), 7.25–7.38 (m, 14H, aromatic ring). MS(FAB), m/z(%): = 367(M^{+1}, 100), 331(75), 307(10), 212(32), 195(5) and 169(6). Electronic spectrum, λ_{max} (cm^{-1}): 39215, 34602, 31695.

2.2. *Synthesis of complexes*

Metal salts used for the preparation of the complexes were obtained from Merck and complexes were prepared according to a method described in the literature [11, 17].

A solution of the metal acetate (0.01 mole) in ethanol (30 cm^3) was added dropwise to a solution of the ligand in a 1 : 2 mol ratio (small excess of ligand) in ethanol (50 cm^3) at room temperature and the resulting mixture was stirred for 30 min. The solid complexes were filtered off and recrystallized from ethanol : dichloromethane (1 : 1).

2.2.1. Bis(*N*,*N*-di-*n*-propyl-*N*′-(2-chlorobenzoyl)thioureato)nickel(II) [Ni(L^1)$_2$]. Red. Yield: 73%, m.p. 114–116°C. Anal. Calcd for $C_{28}H_{36}N_4O_2S_2Cl_2Ni$ (%): C, 51.4; H, 5.6; N, 8.6. Found: C, 51.3; H, 5.6; N, 8.5. IR (cm^{-1}): ν(C=N) 1568 (s), ν(C–Cl) 740 (w). ^{1}H NMR: δ 7.73–7.70 (m, 2H, C_6H_4Cl), 7.30–7.19 (m, 6H, C_6H_4Cl), 3.68–3.60 (m, 8H, N–CH_2), 1.82–1.58 (m, 8H, CH_2), 0.98–0.84 (m, 12H, CH_3). Electronic spectrum, λ_{max} (cm^{-1}): 43668, 34602.

2.2.2. Bis(*N*,*N*-di-*n*-propyl-*N*′-(2-chlorobenzoyl)thioureato)copper(II) [Cu(L^1)$_2$]. Green. Yield: 77%, m.p. 112–114°C. Anal. Calcd for $C_{28}H_{36}N_4O_2S_2Cl_2Cu$ (%): C, 51.0; H, 5.5; N, 8.5. Found: C, 50.6; H, 5.6; N, 8.5 IR (cm^{-1}): ν(C=N) 1572 (s), ν(C–Cl) 749 (w). MS(EI), m/z(%) = 659(M,40), 263(21), 191(26), 139(85), 102(36), 75(27) and 43(100). Electronic spectrum, λ_{max} (cm^{-1}): 35587.

2.2.3. Bis(*N*,*N*-di-*n*-propyl-*N*′-(2-chlorobenzoyl)thioureato)cobalt(II) [Co(L^1)$_2$]. Green. Yield: 75%, m.p. 129–131°C. Anal. Calcd for $C_{28}H_{36}N_4O_2S_2Cl_2Co$ (%): C, 53.0; H, 5.7; N, 8.8. Found: C, 53.1; H, 5.7; N, 8.8 IR (cm^{-1}): ν(C=N) 1567 (s), ν(C–Cl) 744 (w). Electronic spectrum, λ_{max} (cm^{-1}): 35335.

2.2.4. Bis(*N*,*N*-di-*n*-propyl-*N*′-(2-chlorobenzoyl)thioureato)zinc(II) [Zn(L^1)$_2$]. White. Yield: 77%, m.p. 155–157°C. Anal. Calcd for $C_{28}H_{36}N_4O_2S_2Cl_2Zn$ (%): C, 50.9; H, 5.5; N, 8.5. Found: C, 51.5; H, 5.6; N, 8.3. IR (cm^{-1}): ν(C=N) 1574 (s), ν(C–Cl) 748 (w). ^{1}H NMR: δ 7.73–7.70 (m, 2H, C_6H_4Cl), 7.35–7.18 (m, 6H, C_6H_4Cl), 3.79–3.75 (m, 8H, N–CH_2), 1.78–1.64 (m, 8H, CH_2), 1.01–0.89 (m, 12H, CH_3). Electronic spectrum, λ_{max} (cm^{-1}): 43103, 35273.

2.2.5. Bis(*N*,*N*-di-*n*-propyl-*N*′-(2-chlorobenzoyl)thioureato)cadmium(II) [Cd(L^1)$_2$]. Yellow. Yield: 61%, m.p. 170–171°C. Anal. Calcd for $C_{28}H_{36}N_4O_2S_2Cl_2Cd$ (%): C, 47.5; H, 5.1; N, 7.9. Found: C, 48.0; H, 5.2; N, 8.1. IR (cm^{-1}): ν(C=N) 1564 (s), ν(C–Cl) 748 (w). ^{1}H NMR: δ 7.67–7.66 (m, 2H, C_6H_4Cl), 7.28–7.13 (m, 6H, C_6H_4Cl), 3.76–3.56 (m, 8H, N–CH_2), 1.79–1.58 (m, 8H, CH_2), 0.97–0.85 (m, 12H, CH_3). Electronic spectrum, λ_{max} (cm^{-1}): 35587.

2.2.6. Bis(*N*,*N*-di-*n*-propyl-*N*′-(2-chlorobenzoyl)thioureato)platinum(II) [Pt(L^1)$_2$]. Yellow. Yield: 65%, m.p. 155–157°C. Anal. Calcd for $C_{28}H_{36}N_4O_2S_2Cl_2Pt$ (%): C, 42.5; H, 4.6; N, 7.1. Found: C, 43.3; H, 4.7; N, 7.2. IR (cm^{-1}): ν(C=N) 1569 (s), ν(C–Cl) 748 (w). ^{1}H NMR: δ 7.75–7.73 (m, 2H, C_6H_4Cl), 7.31–7.18 (m, 6H, C_6H_4Cl), 3.67–3.61 (m, 8H, N–CH_2), 1.89–1.59 (m, 8H, CH_2), 1.04–0.87 (m, 12H, CH_3). Electronic spectrum, λ_{max} (cm^{-1}): 43668, 40816, 30769.

2.2.7. Bis(*N*,*N*-di-*n*-propyl-*N*′-(2-chlorobenzoyl)thioureato)palladium(II) [Pd(L^1)$_2$]. Yellow. Yield: 79%, m.p. 117–119°C. Anal. Calcd for $C_{28}H_{36}N_4O_2S_2Cl_2Pd$ (%): C, 47.9; H, 5.2; N, 7.9. Found: C, 48.0; H, 5.3; N, 7.8. IR (cm^{-1}): ν(C=N) 1571 (s), ν(C–Cl) 748 (w). ^{1}H NMR: δ 7.73–7.71(m, 2H, C_6H_4Cl), 7.33–7.17 (m, 6H, C_6H_4Cl), 3.70–3.67 (m, 8H, N–CH_2), 1.86–1.63 (m, 8H, CH_2), 1.04–0.88 (m, 12H, CH_3). Electronic spectrum, λ_{max} (cm^{-1}): 36231.

2.2.8. Bis(*N*,*N*-diphenyl-*N*′-(2-chlorobenzoyl)thioureato)nickel(II) [Ni(L^2)$_2$]. Pink. Yield: 70%, m.p. 234–236°C. Anal. Calcd for $C_{40}H_{28}N_4O_2S_2Cl_2Ni$ (%): C, 60.9; H, 3.6; N, 7.1. Found: C, 59.9; H, 3.5; N, 7.2. IR (cm^{-1}): ν(C=N) 1588 (s), ν(C–Cl) 742 (w). ^{1}H NMR: δ 7.16–7.40 (m, 28H, aromatic). Electronic spectrum, λ_{max} (cm^{-1}): 43668, 36832, 32573.

2.2.9. Bis(*N*,*N*-diphenyl-*N*′-(2-chlorobenzoyl)thioureato)copper(II) [Cu(L^2)$_2$]. Brown. Yield: 69%, m.p. 204–206°C. Anal. Calcd for $C_{40}H_{28}N_4O_2S_2Cl_2Cu$ (%): C, 60.4; H, 3.6; N, 7.1. Found: C, 59.3; H, 3.7; N, 6.9. IR (cm^{-1}): ν(C=N) 1576 (s), ν(C–Cl) 749 (w). Electronic spectrum, λ_{max} (cm^{-1}): 43668, 40485, 34013.

2.2.10. Bis(*N*,*N*-diphenyl-*N*′-(2-chlorobenzoyl)thioureato)cobalt(II) [Co(L^2)$_2$]. Green. Yield: 67%, m.p. 230–232°C. Anal. Calcd for $C_{40}H_{28}N_4O_2S_2Cl_2Co$ (%): C, 60.8; H, 3.5; N, 7.1. Found: C, 60.6; H, 3.6; N, 7.2. IR (cm^{-1}): ν(C=N) 1568 (s), ν(C–Cl) 745 (w). Electronic spectrum, λ_{max} (cm^{-1}): 43478, 34965.

2.2.11. Bis(*N*,*N*-diphenyl-*N*′-(2-chlorobenzoyl)thioureato)zinc(II) [Zn(L^2)$_2$]. White. Yield: 78%, m.p. 184–186°C. Anal. Calcd for $C_{40}H_{28}N_4O_2S_2Cl_2Zn$ (%): C, 60.3; H, 3.5; N, 7.0. Found: C, 61.5; H, 3.5; N, 6.9 IR (cm^{-1}): ν(C=N) 1589 (s), ν(C–Cl) 753 (w). ^{1}H NMR: δ 7.41–7.03 (m, 28H, aromatic). Electronic spectrum, λ_{max} (cm^{-1}): 42735, 40567, 34482.

2.2.12. Bis(*N*,*N*-diphenyl-*N*′-(2-chlorobenzoyl)thioureato)cadmium(II) [Cd(L^2)$_2$]. Yellow. Yield: 67%, m.p. 234–236°C. Anal. Calcd for $C_{40}H_{28}N_4O_2S_2Cl_2Cd$ (%): C, 56.9; H, 3.3; N, 6.6. Found: C, 57.2; H, 3.2; N, 6.7. IR (cm^{-1}): ν(C=N) 1574 (s), ν(C–Cl) 748 (w). ^{1}H NMR: δ 7.29–7.25 (m, 28H, aromatic). Electronic spectrum, λ_{max} (cm^{-1}): 43763, 40733, 33500.

2.2.13. Bis(*N*,*N*-diphenyl-*N*′-(2-chlorobenzoyl)thioureato)platinum(II) [Pt(L^2)$_2$]. Yellow. Yield: 61%, m.p. 226–228°C. Anal. Calcd for $C_{40}H_{28}N_4O_2S_2Cl_2Pt$ (%): C, 51.8; H, 3.0; N, 6.1. Found: C, 52.6; H, 2.9; N, 6.2. IR (cm^{-1}): ν(C=N) 1571 (s), ν(C–Cl) 747(w). ^{1}H NMR: δ 7.46–7.12 (m, 28H, aromatic). Electronic spectrum, λ_{max} (cm^{-1}): 43478, 28901.

2.2.14. Bis(*N*,*N*-diphenyl-*N*′-(2-chlorobenzoyl)thioureato)palladium(II) [Pd(L^2)$_2$]. Brown. Yield: 85%, m.p. 276–278°C. Anal. Calcd for $C_{40}H_{28}N_4O_2S_2Cl_2Pd$ (%): C, 57.3; H, 3.4; N, 6.7. Found: C, 58.1; H, 3.5; N, 6.6. IR (cm^{-1}): ν(C=N) 1589 (s),

ν(C–Cl) 748 (w). ^{1}H NMR: δ 7.44–7.11 (m, 28H, aromatic). Electronic spectrum, λ_{max} (cm^{-1}): 43290, 35087.

2.3. *Toxicity studies*

To evaluate cytotoxicity, HEp-2 human cell line ATCC CCL23 was selected. In preparation of the cell cultures, EMEM (Eagle's minimum essential medium) was used with 10% foetal bovine serum (Seromed) as growth medium. Incubation of the cells was performed in an atmosphere of 5% carbon dioxide at 37°C. To determine the effects of the compounds on HEp-2 cells effects of added compound *versus* control cells with no added compound were observed. The non-toxic concentration was determined to be up to 2048 $\mu g\,mL^{-1}$. We used this limit in all experiments to test bacterial growth inhibition. In order to test the effects of the compounds on HEp-2 cells, 5×10^4 cells were seeded into each well of 12-well plates, cultured for 6 h at 28°C, and allowed to grow for an additional 48 h in the presence of increasing amounts of compound (0.5, 1, 2, 4, 8, 16, 32, 64, 128, 256, 512, 1024, 2048 $\mu g\,mL^{-1}$). Cytotoxicity of extracts was determined by a conventional haemocytometer using the trypan blue exclusion method [18]. The highest non-cytocidal (on HEp-2 cells) concentration of the chemical compounds was determined to be 1024 $\mu g\,mL^{-1}$. This limit was used for the determination of antimicrobial activities.

2.4. *Antimicrobial activity*

The compounds were screened for their *in vitro* antibacterial and antifungal activities. Antimicrobial activities were determined by using the agar dilution procedure recommended by the National Committee for Clinical Laboratory Standards [19]. Minimal inhibitory concentrations for each compound were investigated against standard bacterial strains. Activities were tested against the Gram (+) and (−) bacteria *Escherichia coli* ATCC 25922, *Enterobacter cloacae* ATCC 13047, *Enterococcus faecalis* ATCC 29212, *Pseudomonas aeruginosa* ATCC 27853, *Staphylococcus aureus* ATCC 29213 and *Staphylococcus epidermidis* ATCC 12228, and yeast-like fungi *Candida albicans* (ATCC 90028), *Candida krusei* (ATCC 6258), *Candida parapsilosis* (ATCC 22019), *Candida tropicalis* (ATCC 22019) and *Candida glabrata* (ATCC 32554), obtained from the Department of Microbiology, Faculty of Medicine, Ege University, Turkey. Minimal inhibitory concentrations were determined by the broth microdilution method following the procedures recommended by the National Committee for Clinical Laboratory Standards [20].

Stock solutions were prepared in dimethyl sulfoxide (DMSO) and DMSO had no effect on the microorganisms at the concentration used. All dilutions were done with distilled water. The concentrations of tested compounds were 1024, 512, 256, 128, 64, 32, 16, 8, 4, 2 and 1 $\mu g\,cm^{-3}$. Fluconazole and amikacin sulphate were used as reference drugs for antifungal and antibacterial activities, respectively. A loop (0.01 cm^3) of the standardised inoculum of the bacteria and fungi (10^6 CFUs cm^{-3}) was spread over the surface of agar plates. All inoculated plates were incubated at 35°C and results were evaluated after 16–20 h for bacteria and 48 h for fungi. The lowest concentration of the compounds that prevented visible growth was considered to be the minimal inhibitory concentration (MIC).

3. Results and discussion

Electronic spectra of the ligands show two strong absorption bands (236 and 287 nm for HL^1 and 255 and 289 nm for HL^2) in the UV region. The first can be assigned to a $\pi \rightarrow \pi^*$ intraligand transition. In the metal complexes, bands below ~340 nm are attributed to intraligand transitions [21]. A small shift should be observed for the second band in all complexes, these $\pi \rightarrow \pi^*$ transitions probably involving metal and ligand orbitals. Bands above ~340 nm are ascribed to charge transfer processes, probably from ligand to metal and mainly associated with the N–C=S and N–C=O groups, since the Zn(II) and Cd(II) complexes do not show these transitions. Absorption bands at higher wavelengths are due to d–d transitions [17, 21]. Characteristic IR bands are given in experimental section. The medium peak (3138 for HL^1 and 3158 cm^{-1} for HL^2) is attributed to stretching of the N–H group adjacent to the carbonyl group and this disappears in the complexes. A strong absorption (1690 for HL^1 and 1694 cm^{-1} for HL^2) is ascribed to the stretching vibrational of the carbonyl groups and shifts upon complexation. Deprotonation induces delocalization of C=O stretching vibration (~180 cm^{-1} decrease) in agreement with the literature [11, 21] and confirming coordination through oxygen. A large decrease should also be observed for the C=S stretch, but this vibration could not be located in the spectra of the complexes. IR spectra of the complexes are similar. ^{1}H NMR spectra of compounds show aromatic protons with slight variations in position. Aryl proton signals are shifted to lower field (0.1–0.2 ppm) relative to those in the free ligands. Methylene protons of the propyl group show two signals at *ca* 3.9 and 3.6 ppm. HL^1 and HL^2 show a peak at 8.76 and 8.86 ppm, respectively, corresponding to the proton of the N–H group. This is not seen in the

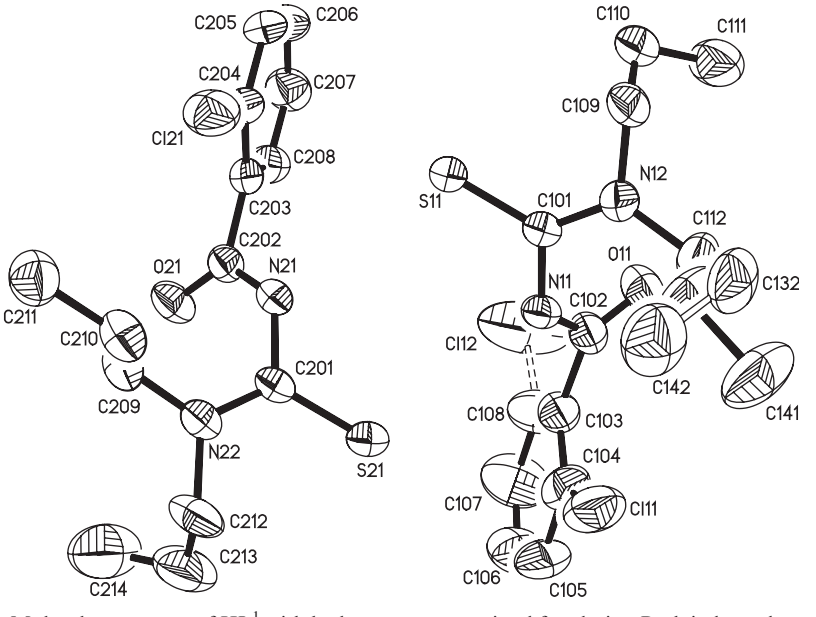

Figure 1. Molecular structure of HL^1 with hydrogen atoms omitted for clarity. Both independent molecules are shown with thermal ellipsoids drawn at the 50% probability level.

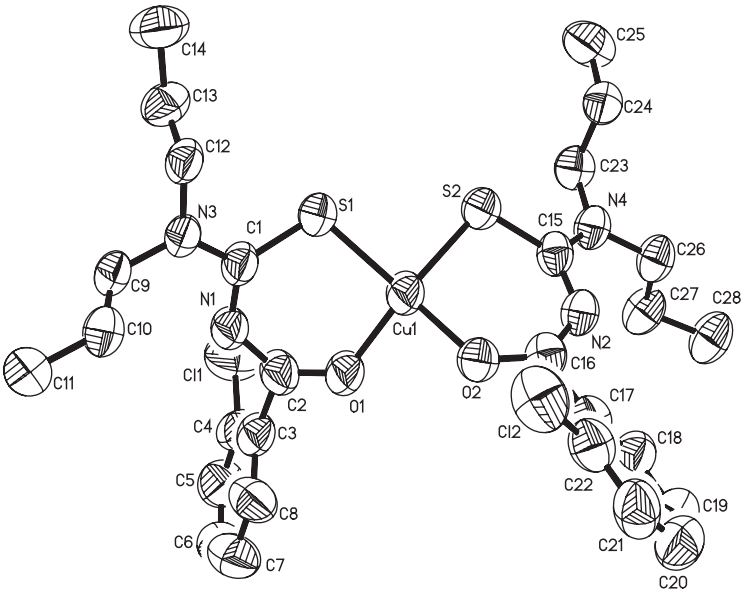

Figure 2. Molecular structure of $Cu(L^1)_2$ with hydrogen atoms omitted for clarity. Thermal ellipsoids are drawn at the 50% probability level.

Table 2. Selected bond lengths (Å) and angles (°), for HL^1 average values for molecules $x = 1$ and $x = 2$.

Compound				
HL^1	Bond lengths			
	N(x2)–C(x12)	1.472(7)	C(x01)–N(x1)	1.407(6)
	N(x2)–C(x01)	1.331(6)	C(x02)–N(x1)	1.366(6)
	N(x2)–C(x09)	1.486(7)	C(x02)–C(x03)	1.507(7)
	C(x01)–S(x1)	1.671(5)	C(x02)–O(x1)	1.221(6)
	Bond angles			
	C(x09)–N(x2)–C(x12)	116.4(4)	C(x02)–N(x1)–C(x01)	125.1(4)
	N(x2)–C(x01)–N(x1)	117.2(4)	C(x01)–N(x2)–C(x12)	122.0(5)
	N(x1)–C(x02)–C(x03)	113.1(4)	C(x01)–N(x2)–C(x09)	121.1(4)
	Cu(1)–S(1)	2.225(3)	S(1)–C(1)	1.741(10)
$Cu(L^1)_2$	Bond lengths			
	Cu(1)–O(1)	1.931(7)	C(1)–N(1)	1.345(11)
	N(1)–C(2)	1.315(12)	C(1)–N(3)	1.323(11)
	C(2)–O(1)	1.281(12)	S(2)–C(15)	1.741(9)
	Cu(1)–S(2)	2.246(3)	N(2)–C(15)	1.330(12)
	Cu(1)–O(2)	1.913(7)	N(2)–C(16)	1.319(12)
	O(2)–(16)	1.283(11)	C(15)–N(4)	1.331(12)
	Bond angles			
	O(1)–Cu(1)–S(1)	95.2(2)	C(2)–N(1)–C(1)	125.4(8)
	S(1)–Cu(1)–S(2)	90.89(11)	C(15)–N(2)–C(16)	125.7(8)
	O(2)–Cu(1)–S(2)	94.0(2)	C(1)–S(1)–Cu	105.7(3)
	O(2)–Cu(1)–O(1)	86.9(3)	C(2)–O(1)–Cu	127.4(7)
	O(1)–Cu(1)–S(2)	158.2(3)	C(15)–S(2)–Cu	103.8(3)
	O(2)–Cu(1)–S(1)	161.2(2)	C(16)–O(2)–Cu	130.2(7)

complexes [11], in agreement with the IR spectra. Magnetic susceptibilities values indicate that Ni(II), Pd(II), Pt(II), Cd(II) and Zn(II) complexes are diamagnetic, while Cu(II) and Co(II) complexes are paramagnetic. The measured values for the $Cu(L^1)_2$, $Cu(L^2)_2$, $Co(L^1)_2$ and $Co(L^2)_2$ complexes are 1.76, 1.80, 3.85 and 3.91 BM, respectively. The complexes have a distorted square planar structure, in agreement with other literature data [11, 13, 22, 23].

Some metal complexes were studied by thermogravimetric methods from ambient temperatures to 1000 K. Traces for most of the compounds were very similar. The first mass loss corresponds to the formation of their respective thiocyanates while the second mass loss is due to the decomposition of thiocyanate. End products were confirmed with XRD data. As an example, X-ray powder diffraction studies for $Co(L^2)_2$ showed that the residual solid was Co_4S_3, which corresponds to a theoretical residual mass of 10.5%. TG gave an end-product mass of 10.2%. According to X-ray patterns, pyrolytic end products of relevant metal complexes are Pd, Pt, $Cu_{1.96}S$, Ni_3S_2 and Co_4S_3, in agreement with literature data [2, 6, 15].

The molecular structures of *N*,*N*-di-*n*-propyl-*N*′-(2-chlorobenzoyl)thiourea and *cis*-bis(***N***,***N***-di-*n*-propyl-*N*′-(2-chlorobenzoyl)thiourea)copper(II) are depicted in figures 1 and 2, respectively. Selected bond lengths and angles are listed in table 2.

Table 3. MIC values and toxicity assays for yeast-like fungi.

	MIC values (lower 95% lim–upper 95% lim) $\mu g\,cm^{-3}$				
Compound	*C. albicans*	*C. krusei*	*C. parapsilosis*	*C. tropicalis*	*C. glabrata*
$Pt(L^1)_2$	224 ± 64 (122–326)	160 ± 64 (58–262)	320 ± 128 (116–524)	160 ± 64 (58–262)	224 ± 64 (122–326)
$Pd(L^1)_2$	224 ± 64 (122–326)	320 ± 128 (116–524)	224 ± 64 (122–326)	224 ± 64 (122–326)	384 ± 148 (149–619)
$Cd(L^1)_2$	320 ± 128 (116–524)	384 ± 148 (149–619)	448 ± 128 (224–652)	288 ± 161 (32–544)	224 ± 64 (122–326)
$Zn(L^1)_2$	384 ± 148 (149–619)	448 ± 128 (224–652)	288 ± 161 (32–544)	160 ± 64 (58–262)	384 ± 148 (149–619)
$Co(L^1)_2$	320 ± 128 (116–524)	288 ± 161 (32–544)	448 ± 128 (224–652)	288 ± 161 (32–544)	320 ± 128 (116–524)
$Ni(L^1)_2$	224 ± 64 (122–326)	448 ± 128 (224–652)	384 ± 148 (149–619)	160 ± 64 (58–262)	224 ± 64 (122–326)
$Cu(L^1)_2$	224 ± 64 (122–326)	320 ± 128 (116–524)	224 ± 64 (122–326)	224 ± 64 (122–326)	320 ± 128 (116–524)
$Pt(L^2)_2$	175.0 ± 50.0 (95–255)	250 ± 37 (158–342)	150 ± 58 (58–242)	225 ± 50 (146–305)	250 ± 37 (158–342)
$Pd(L^2)_2$	175 ± 50 (95–255)	250 ± 37 (158–342)	225 ± 50 (146–305)	225 ± 50 (146–306)	225 ± 50 (146–305)
$Cd(L^2)_2$	175 ± 50 (95–255)	175 ± 50 (95–255)	150 ± 58 (58–242)	150 ± 58 (58–242)	225 ± 50 (146–305)
$Zn(L^2)_2$	225 ± 50 (146–305)	175 ± 50 (95–255)	175 ± 50 (95–255)	225 ± 50 (146–305)	225 ± 50 (146–305)
$Co(L^2)_2$	250 ± 37 (158–342)	150 ± 58 (58–242)	150 ± 58 (58–242)	250 ± 37 (158–342)	150 ± 58 (58–242)
$Ni(L^2)_2$	225 ± 50 (146–305)	225 ± 50 (146–305)	175 ± 50 (95–255)	225 ± 50 (146–305)	225 ± 50 (146–305)
$Cu(L^2)_2$	225 ± 50 (146–305)	150 ± 58 (58–242)	250 ± 37 (158–342)	250 ± 37 (158–342)	250 ± 37 (158–342)
Flucanazole	1.3 ± 0.6 (0.1–2.8)	13.3 ± 4.6 (1.9–24.8)	2.7 ± 1.2 (0.2–5.5)	3.3 ± 1.2 (0.5–6.2)	3.0 ± 1.2 (1.2–4.8)

Table 4. MIC values and toxicity assays for bacteria.

Compound	MIC value (lower 95% lim–upper 95% lim) $\mu g\,cm^{-1}$					
	E. coli	*E. cloacae*	*E. faecalis*	*P. aeruginosa*	*S. aureus*	*S. epidermidis*
$Pt(L^1)_2$	160 ± 64 (58–262)	160 ± 64 (58–262)	107 ± 37 (15–199)	2058 ± 70 (118–292)	85 ± 37 (7–177)	53 ± 19 (7–99)
$Pd(L^1)_2$	107 ± 37 (15–199)	224 ± 64 (122–326)	171 ± 74 (13–345)	171 ± 74 (13–345)	107 ± 37 (15–199)	85 ± 37 (7–177)
$Cd(L^1)_2$	144 ± 81 (16–272)	107 ± 37 (15–199)	107 ± 37 (15–199)	205 ± 70 (118–292)	171 ± 74 (13–345)	107 ± 37 (15–199)
$Zn(L^1)_2$	160 ± 64 (58–262)	160 ± 64 (58–262)	96 ± 37 (37–155)	224 ± 64 (122–326)	85 ± 37 (7–177)	53 ± 19 (7–99)
$Co(L^1)_2$	171 ± 74 (13–345)	205 ± 70 (118–292)	224 ± 64 (122–326)	144 ± 81 (16–272)	107 ± 37 (15–199)	85 ± 37 (7–177)
$Ni(L^1)_2$	144 ± 81 (16–272)	171 ± 74 (13–345)	85 ± 37 (7–177)	205 ± 70 (118–292)	171 ± 74 (13–345)	53 ± 19 (7–99)
$Cu(L^1)_2$	160 ± 64 (58–262)	107 ± 37 (15–199)	107 ± 37 (15–199)	171 ± 74 (13–345)	96 ± 37 (37–155)	85 ± 37 (7–177)
$Pt(L^2)_2$	88 ± 14 (65–111)	150 ± 58 (58–242)	94 ± 13 (74–114)	175 ± 50 (95–255)	75 ± 29 (29–121)	75 ± 29 (29–121)
$Pd(L^2)_2$	150 ± 58 (58–242)	94 ± 13 (74–114)	94 ± 13 (74–114)	94 ± 13 (74–114)	63 ± 25 (23–102)	94 ± 13 (74–114)
$Cd(L^2)_2$	175 ± 50 (95–255)	150 ± 58 (58–242)	94 ± 13 (74–114)	150 ± 58 (58–242)	75 ± 29 (29–121)	94 ± 13 (74–114)
$Zn(L^2)_2$	150 ± 58 (58–242)	150 ± 58 (58–242)	75 ± 29 (29–121)	175 ± 50 (95–255)	63 ± 25 (23–102)	75 ± 29 (29–121)
$Co(L^2)_2$	150 ± 58 (58–242)	94 ± 13 (74–114)	947 ± 13 (74–114)	94 ± 13 (74–114)	63 ± 25 (23–102)	63 ± 25 (23–102)
$Ni(L^2)_2$	175 ± 50 (95–255)	175 ± 50 (95–255)	94 ± 13 (74–114)	175 ± 50 (95–255)	75 ± 29 (29–121)	44 ± 13 (24–64)
$Cu(L^2)_2$	947 ± 13 (74–114)	94 ± 13 (74–114)	94 ± 13 (74–114)	150 ± 58 (58–242)	75 ± 29 (29–121)	63 ± 25 (23–102)
Amik.	1.25 ± 0.5 (0.5–2.0)	3.3 ± 1.2 (0.5–6.2)	27 ± 9 (3.7–49.6)	2.7 ± 1.2 (0.2–5.5)	4.7 ± 1.2 (1.8–7.5)	5.3 ± 2.3 (0.4–11.1)

The crystal structure of HL^1 consists of two independent molecules per asymmetric unit, both with same conformation, but molecule 1 shows disorder of the C(13) and C(14) positions of one propyl group over two sites with site occupancy factors of 0.516(5) and 0.484(5). Additionally, the 2-chlorobenzoyl group of the same molecule is disordered along the C(102)–C(103) axis resulting in split positions for the Cl atom with site occupancy factors of 0.57(1) and 0.43(1). The overall molecular structure of HL^1 is similar to that of *N*′-(2-chlorobenzoyl)-*N*-(pyrrolidin-1-yl)thiourea [24] apart from the *N*-pyrrolidine group.

$Cu(L^1)_2$ shows the Cu ion is four-coordinated by two O and two S atoms (S(1)–Cu–O(2) 161.2(2)°, O(1)–Cu–S(2) 158.2(3)°). The dihedral angle between the S(1)CuO(1) and S(2)CuO(2) planes of 27.7(1)° indicates strong distortion from square planar towards tetrahedral geometry. With respect to the chelating ligands the molecule shows a *cis*-arrangement. Bond lengths of the carbonyl groups are C(2)–O(1) 1.281(12) and C(16)–O(2) 1.28311) Å; corresponding thiocarbonyl bondlengths, C(1)–S(1) 1.741(10) and C(15)–S(2) 1.741(9) Å, lie between those typical of double and single bonds, a feature known from related structures [11, 15, 25]. Similar observations are true for the C–N bonds. This is due to strong delocalisation in the chelate ring. All other bond lengths fall within expected ranges.

Safety tests including cytotoxicity assays are required for all products to be used in contact with humans. Cytotoxicity tests using culture cells have been accepted as a first step in identifying active compounds and for biosafety testing. Samples were placed in contact with a monolayer of HEp-2 cells and incubated. The cells were then scored for cytopathic effects [26, 27]. The compounds were then screened for antimicrobial activity at non-toxic concentrations. Compounds were screened for *in vitro* antibacterial and antifungal activities. The results obtained are given in tables 3 and 4. All compounds inhibited the growth of bacteria at MIC values between 43 and 224 $\mu g\,cm^{-3}$ and showed antifungal activity with MICs between 150 and 448 $\mu g\,cm^{-3}$. The lowest MIC values against *Staphylococcus epidermidis* were obtained with $Ni(L^2)_2$. Lowest MIC values against growth of *Candida parapsilos* were obtained with Pt, Cd and Co complexes of HL^2.

All compounds showed antimicrobial activity, but antibacterial efficacy is higher than antifungal activity. Antimicrobial activity against bacteria may depend on the difference between cell structures of bacteria and fungi. The cell walls of fungi contain chitin, which add rigidity and structural support. In addition, fungi contain ergosterol in of cell membrane instead of cholesterol in the cell membrane of animals [28].

Supplementary material

Crystallographic data for the structures reported in this paper have been deposited at the Cambridge Crystallographic Data Centre (CCDC), CCDC 189043 for L^1H and CCDC 189045 for $Cu(L^1)_2$, and can be obtained free of charge on application to CCDC, 12 Union Road, Cambridge CB2 1EZ, UK [Fax: +44 1223 336033, E-mail: deposit@ccdc.cam.ac.uk].

Acknowledgements

This work was supported by the Mersin University Research Fund (Project Nos: BAP.ECZ.TB.HA.2004-3 and BAP.FEF.KB.NK.2002,2004-2,2005-1).

References

[1] L. Beyer, J.J. Criado, E. Garcia, F. Lessmann, M. Medarde, R. Richter, E. Rodriguez. *Tetrahedron*, **52**, 6233 (1996).
[2] H. Arslan, N. Ozpozan, T. Ozpozan. *Thermochimica Acta*, **329**, 57 (1999).
[3] N. Ozpozan, T. Ozpozan, H. Arslan, F. Karipcin, N. Külcü. *Thermochimica Acta*, **336**, 97 (1999).
[4] N. Ozpozan, H. Arslan, T. Ozpozan, N. Ozdes, N. Külcü. *Thermochimica Acta*, **343**, 127 (2000).
[5] N. Ozpozan, H. Arslan, T. Ozpozan, M. Merdivan, N. Külcü. *J. Therm. Anal.*, **61**, 955 (2000).
[6] G. Avşar, N. Külcü, H. Arslan. *Turk. J. Chem.*, **26**, 607 (2002).
[7] F.A. French, E.J. Blanz, J.R.D. Amaral, D.A. French. *J. Med. Chem.*, **13**, 1117 (1970).
[8] R. Campo, J.J. Criado, R. Gheorghe, F.J. González, M.R. Hermosa, F. Sanz, J.L. Manzano, E. Monte, E. Rodríguez-Fernández. *J. Inorg. Biochem.*, **98**, 1307 (2004).
[9] W. Antholine, F. Taketa. *J. Inorg. Biochem.*, **16**, 145 (1982).
[10] H. Arslan, U. Flörke, N. Kulcu. *Acta Cryst.*, **E59**, organic 641 (2003).

[11] H. Arslan, U. Flörke, N. Kulcu. *Trans. Metal Chem.*, **28**(7), 816 (2003).
[12] H. Arslan, U. Flörke, N. Kulcu. *J. Chem. Crystallog.*, **33**, 919 (2003).
[13] H. Arslan, D. Vanderveer, F. Emen, N. Külcü. *Z. Kristallogr. NCS.*, **218**, 479 (2003).
[14] H. Arslan, U. Flörke, N. Kulcu. *Acta Chim. Slovenica*, **51**, 787 (2004).
[15] H. Arslan, U. Flörke, N. Kulcu, M.F. Emen. *J. Coord. Chem.*, **59**(2), 223 (2006).
[16] G.M. Sheldrick. *SHELXTL v. 5.1, Structure Determination Software Suite*, Bruker AXS, Madison, Wisconsin, USA (1998).
[17] G. Polat. MSc thesis, Mersin University, Mersin, Turkey (2003).
[18] F.G. Burlesson, T.M. Chambers, D.L. Wedbrauk. *Virology, A Laboratory Manual*, Academic Press, New York (1992).
[19] National Committee for Clinical Laboratory Standards (NCCLS). *Methods for Dilution Antimicrobial Susceptibility Tests for Bacteria that Grow Aerobically*, Approved Standard M7-A2, NCCLS Villanova, PA (1997).
[20] National Committee for Clinical Laboratory Standards (NCCLS). *Reference Method for Broth Dilution Antifungal Susceptibility Testing of Yeasts*, Proposed Standard. Document M27-P. NCCLS, Villanova, PA (1992).
[21] M. Mikami, I. Nakagawa, T. Shimanouchi. *Spectrochim. Acta*, **23A**, 1037 (1967).
[22] G. Avsar, H. Arslan, H.-J. Haupt, N. Külcü. *Turk. J. Chem.*, **27**, 281 (2003).
[23] R.L. Duta, A. Syamal, *Elements of Magnetochemistry*, Elsevier Press, New Delhi (1992).
[24] F.M. Emen, U. Flörke, N. Külcü, H. Arslan. *Acta Cryst.*, **E59**, organic 1159 (2003).
[25] R.A. Bailey, K.L. Rothaupt, R.K. Kullnig. *Inorg. Chim. Acta*, **147**, 233 (1988).
[26] E. Borenfreund, J.A. Puerner. *Toxicology Lett.*, **24**, 119 (1985).
[27] E. Borenfreund, J.A. Puerner. *J. Tissue Culture Methods*, **9**, 7 (1984).
[28] G.H. Fleet. *Composition and Structure of Yeast Cell Walls: Current Topics in Medical Mycology*, Vol. 1, Springer-Verlag, New York (1985).